MODELING THE CROSS-SECTION OF FINNED-TUBE HEAT EXCHANGERS FOR LATENT HEAT THERMAL ENERGY STORAGE SYSTEMS USED IN CARNOT BATTERIES

Matias Pezo*, Wolf-Dieter Steinmann, Andrea Gutierrez

[1] Institute of Engineering Thermodynamics, German Aerospace Center (DLR), Pfaffenwaldring 38-40, 70569 Stuttgart, Germany

*Corresponding Author: matias.pezoperez@dlr.de

ABSTRACT

Carnot Batteries are proposed as a solution for the dispatchability problem caused by the growth of fluctuating renewable energy sources. Here, Thermal Energy Storages are combined with thermal power cycles to store electrical energy. In Carnot Battery concepts based on steam power cycles, Latent Heat Thermal Energy Storages (LHTES) are essential components due to their ability to reach high energy densities in a narrow temperature gap thus, allowing nearly isothermal charge and discharge. In LHTES systems, usually storage materials with low thermal conductivities are applied, the identification of effective solutions to transfer heat between the storage material undergoing a phase change and the working fluid is a key challenge, therefore, the development of simulation tools for the analysis of LHTES on different scales is essential for their application in Carnot Batteries

This paper analyses the charge and discharge behavior of four different longitudinal finned-tube heat-exchanger geometries with common fin fraction, as an initial step for the development of a multi-scale simulation tool for the integration of LHTES in Rankine-based Carnot Batteries.

Each fin geometry is analyzed numerically using COMSOL Multiphysics on a two-dimensional model, to obtain their characteristic charge and discharge curves, specifically in terms of the Phase Change Material (PCM) liquid fraction and the heat flux over a given period. A high-melting-temperature PCM eutectic mixture of KNO_3-$NaNO_3$ with a melting temperature of 222 °C was selected.

Alternative geometric and thermal performance parameters were proposed as a framework to compare the finned-tube heat exchanger designs. To determine the effectiveness of the proposed parameters to describe each geometry, a correlation between the parameters and the phase change time was made. The average minimum distance (AD_{min}) between the fin and PCM presented a better correlation compared to the contact perimeter between fins and PCM. Profiles with lower AD_{min} exhibited higher heat fluxes and lower discharge times due to better material distribution.

The insights gained from this study will be applied to the development of an equivalent resistance model based on the characteristic curves of each fin geometry. This model will be experimentally validated using a currently under-construction test rig.

1 INTRODUCTION

The increasing share of fluctuating renewable energy sources coupled with increasing global energy demand has focused engineering interest on new forms of energy storage (IEA, 2024). Among the various power-to-power technologies, Carnot Batteries store electrical energy into thermal energy using three main components: a heat source, a power cycle and a thermal energy storage unit (Vandersickel et al., 2023). In comparison to pumped hydro and lithium-ion batteries, Carnot Batteries do not have geological or resource constraints, delivering a high number of cycles with a small environmental impact (Dumont et al., 2020).

Thermal energy can be stored using sensible, latent, or thermochemical methods. On narrow temperature differences, Latent Heat Thermal Energy Storage (LHTES) has a higher energy density in comparison to the sensible approach. LHTES Systems use Phase Change Materials (PCMs) as a storage medium, where the solid-liquid is the preferred phase transition since it allows storage at ambient pressure with low-density variations between phases (Li et al., 2021).

Among the passive LHTES concepts, the shell-and-tube approach has reached the highest maturity. Here, the PCM mass is contained by the shell, and tubes are used to charge and discharge thermal energy using a Heat Transfer Fluid, short HTF. This study will use the vertical staggered tube layout since it prevents isolated liquid volumes by ensuring that the melting progresses from the top to the bottom during charging, and solidification occurs from the bottom up during discharging (Steinmann, 2022).
PCMs can be classified based on their chemical composition, melting temperature and energy storage capabilities. Inorganic salts have relatively high energy densities and industrially compatible melting temperatures. Nevertheless, cost-effective PCMs have low thermal conductivities, limiting the energy input and output of the storage. To overcome this challenge, the contact area of the tubes is extended using aluminum fins (Mehling, 2008). Fins can be classified depending on their design as annular/parallel or longitudinal/axial fins. Figure 1 shows two categories of the most commonly used fin designs in the literature, which have been thoroughly reviewed by previous studies (Zayed et al., 2020; Zhang et al., 2023; Zhu et al., 2023). Former studies have shown that independent of the geometry, fins represent between 30 and 40% of the capital costs of the LHTES module, making them a crucial optimization aspect (DLR, 2012).

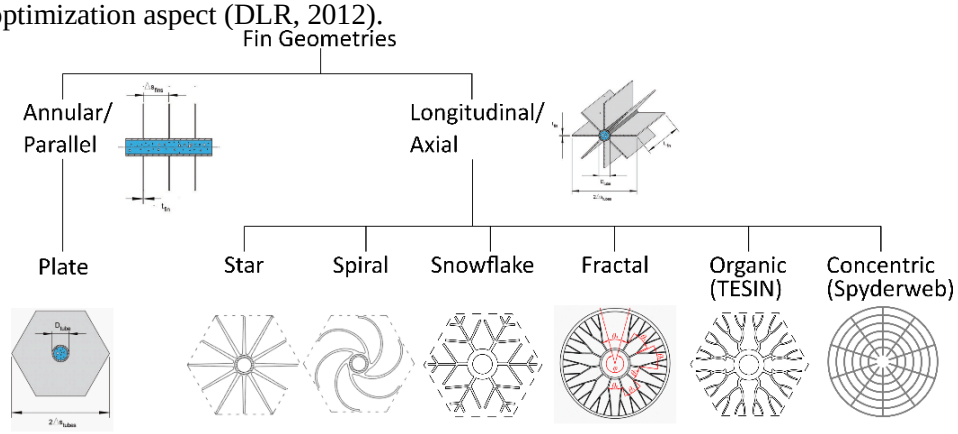

Figure 1: Classification of different fin geometries.

Although the PCM modeling literature is vast, there are few studies considering the effect of the design of the finned structure on the full storage performance. Most of the studies focused on the cross-section of the PCM heat exchanger do not scale their results to develop a model describing a multi-tube storage unit.
The effects of natural convection are often neglected although their importance depends strongly on the used layout and fin design. Vogel and Johnson (2019) used numerical simulations to evaluate the effect of fin design and tube length on four different fin profiles using $NaNO_3$ as PCM. One of them (axial 230) was evaluated for three different fin heights to measure the effects of this parameter on natural convection. Their results showed non-neglectable effects for geometries with large tube spacing and low fin fraction, whereas for configurations with small tube spacing, high fin fraction and short tube lengths, natural convection was found negligible. Vogel et al. (2020) developed a less computationally expensive LHTES-calculation tool calibrated with an ANSYS Fluent model. The tool used an effective material of PCM and fins to reduce the number of elements where the differential equations had to be solved. The properties of the effective material were calculated following the factor of parallelism proposed by Tay et al. (2012), to describe how parallel or in series the heat was transferred. The calculation of this factor requires previous CFD or experimental calibration, which is very time-consuming when a wide variety of fin designs are evaluated. Furthermore, even though the results delivered by the tool were accurate, the model could be simplified for faster calculations considering a quasi-stationary state, and therefore, not having to solve the differential equations describing the PCM volume.
Sciacovelli et al. (2015) studied two types of fractal (Y-fin) designs with single and double bifurcations on a vertical layout. The geometry was parametrically optimized using the length and bifurcation angles, maintaining the cross-sectional area of the fin to maximize the heat flux given an operating time constraint.

Pizzolato et al. (2017a) introduced a methodology to obtain 2D topologically optimized fins on a horizontal layout assessing both, melting and solidification processes, and comparing the results considering non-neglectable and neglectable natural convection. Because of the chosen layout, the resulting fins do not have an even distribution of the fin material, they instead follow non-trivial paths to reduce the solidification time. The study of topologic finned structures continued assessing the 3D branch distribution of the topologically optimized fins by Pizzolato et al. (2017b). Two minimization approaches were proposed, first the residual energy of the storage after a given time, and second the solidification time. Although the 3D results outperformed those of the 2D approach, the high complexity of the obtained structures makes it impossible to manufacture them without additive manufacturing techniques, which currently are too costly for applications at industrial scale. Ge et al. (2020) studied arrays of four finned tubes, comparing topologically optimized fins to star fins using CFD simulations, and experimentally using 3D printed fins and an acrylic shell. Three different paraffins with melting temperatures below 30 °C were used as PCMs. The topological fin had shorter solidification times but the star profile used as a benchmark was not optimized. Wang et al. (2023) compared a variety of star and topologically optimized fin profiles for the melting of a paraffin-based PCM. For the optimization, the heat transfer during phase change was maximized. While maintaining the same fin material for all profiles, the topological approach presented slightly shorter melting times than the best-performing star profile. When the fin fraction was increased, the melting time decreased but so did the storage capacity because of the lower PCM mass.

Table 1 summarizes the characteristics of the above-mentioned investigations. As a general conclusion, most of the above studies lack systematic analysis of parameters to characterize the fin profiles for a storage unit simulation tool.

Table 1: Summary of investigations cited in the introduction.

Study	**PCM (T_m [°C])**	**PC***	**Type of fin**	**Layout**
Vogel and Johnson (2019)	$NaNO_3$ (306)	S&M	A (TESIN, Snowflake, Star) & P (Plates)	V-ST
Vogel et al. (2020)	$NaNO_3$ (306) KNO3- $NaNO_3$ (222)	S&M	A (TESIN) & P (Plates)	V-ST
Sciacovelli et al. (2015)	Paraffin wax (57)	S	A (Fractal)	V-ST
Pizzolato et al. (2017a)	Dimensionless PCM (-)	S	A (2D Top. opt.)	H-ST
Pizzolato et al. (2017b).	Dimensionless PCM (-)	S	A (2D Top. opt.) & O (3D Top. opt.)	V-ST
Ge et al. (2020)	3 paraffins: RT18HC (18), RT22HC (22), RT25HC (24)	S	A (2D Top. opt. & 10-Branch-Star)	V-TA
Wang et al. (2023)	RT50 Paraffin (51)	M	A (Star & 2D Top. opt.)	H-ST

**Studied Phase Change (PC) can either be Solidification (S), Melting (M), or both (S&M). The type of fin can either be Axial (A), Parallel (P) or Other (O). The layout can be Vertical (V), Horizontal (H) combined with the assessment of a Single Tube (ST) or Tube Arrays (TA).*

This paper focuses on the modeling of the cross-section of four different fin profiles using the same fin fraction to evaluate how the distribution of the fin material affects the phase change. The main objective of this paper is to further characterize the finned structures considering geometrically based parameters and thus, enable the reduction of computational costs for the calculations. The eutectic mixture of KNO_3 -$NaNO_3$ with a melting temperature of 222 °C will be used as PCM. The characterization results will be used as a first step for the development of a multi-scale simulation tool shown in Figure 2, which describes three different levels that compose the LHTES module. The third level represents the modeling of the storage unit with multiple tubes, the second level represents a single tube of length up

to six meters, and the first level corresponds to the cross-section of the heat exchanger using different fin geometries with only 15 mm of tube length.

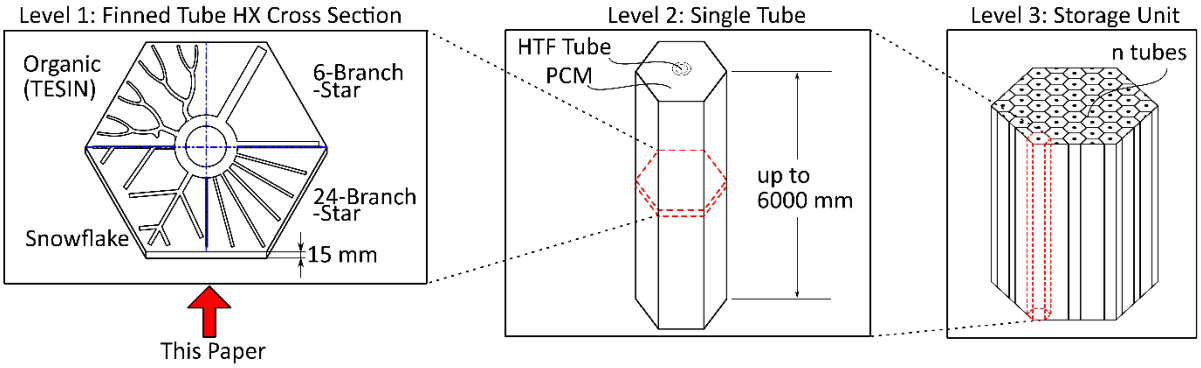

Figure 2: Hierarchical Multi-Scale Modelling Approach.

2 METHODOLOGY

The commercial simulation tool COMSOL-Multiphysics® (2025) was used for the simulation. The Heat Transfer and CAD-Import modules were used to carry out a time-dependent study of the melting and solidification. Table 2 shows the thermophysical properties of the eutectic mixture of KNO_3-$NaNO_3$ used as PCM, and the aluminum used for the fin and tube.

Table 2: Thermophysical properties of PCM and aluminum.

Property	Solid PCM	Liquid PCM	Al6060
Th. Conduct. [W m^{-1} K^{-1}]	0.435	0.457	210
Heat Capacity [J kg^{-1} K^{-1}]	1350	1492	1020
Density [kg m^{-3}]	2017.5		2700
Melting Temperature [°C] ([K])	222 (495.15)		-
Latent Heat [kJ kg^{-1}]	108		-

On the 2D plane, the fin fraction can be calculated as shown in Equation (1), which is the ratio between the cross-sectional fin area A_{fin} to the total hexagon area A_{hex}:

$$f_{fin} = \frac{A_{fin}}{A_{hex}} = \frac{A_{fin}}{A_{fin} + A_{PCM} + A_{tube}} \quad (1)$$

2.1 Description of the numerical model

In this context, Figure 3 shows the four fin designs considered for this study, all of them with the same fin fraction, only differing on the distribution of the aluminum material. To reduce the computational time for assessing the complete fin design on COMSOL, symmetry was used to obtain the simplified structure shown on the right of each fin profile. At the start, the whole system was considered to be at the same temperature, either 10 K above the melting temperature for the solidification study, or 10 K below the melting temperature for the solid-liquid phase change. Then, a temperature boundary condition (212 °C for solidification, 232 °C for melting) was applied on the inner tube border (blue edge in Figure 3).

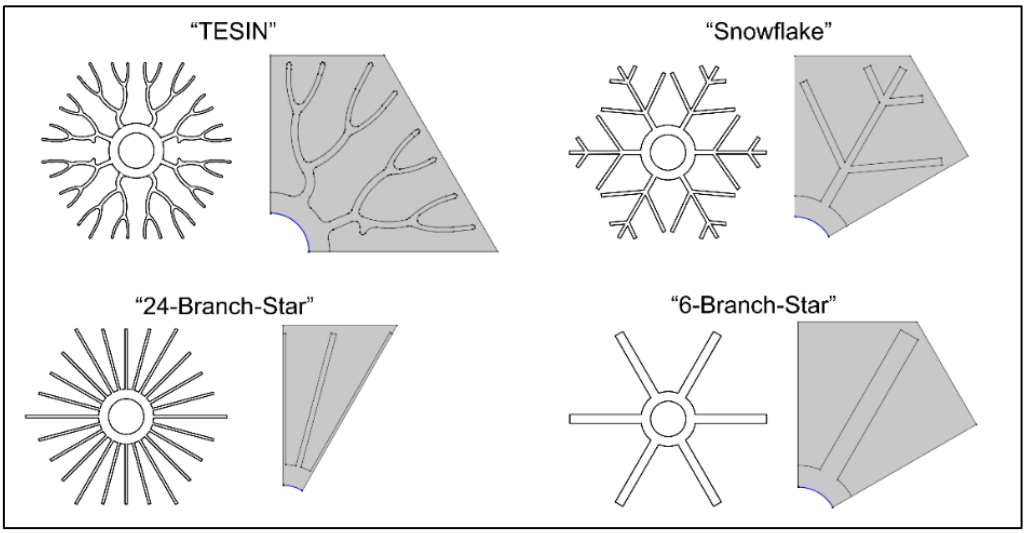

Figure 3: Cross-section of the studied finned-tube heat exchangers and simplified geometry used in COMSOL.

The following assumptions were made to simplify the resolution of the Navier-Stokes equations:

- Isentropic conduction-based heat transfer. Radiation and convection are neglected.
- Latent heat, melting temperature and density are considered constant.
- Phase change interface is locally planar and sharp.
- Thermal conductivity and heat capacity are considered constant for each phase.
- Density is considered constant to avoid variations in the mass of the PCM control volume
- For the boundary condition, phase change of the heat transfer fluid is assumed. Hence a constant temperature in the inner wall will be considered

The cross-section analyzed in this paper is part of a PCM volume integrated with a heat exchanger formed by an arrangement of finned tubes. Since the orientation of the tubes is vertical, two components are expected to be relevant for natural convection; first, the relative position across the tube length, and second, the interaction with neighboring finned tubes affected by external boundary conditions. The analysis of natural convection would require the calculation of at least one pipe over the entire length, which would lead to considerable computational efforts if a typical length of 6 meters is calculated. In addition, the influence of natural convection during solidification is estimated to be low. For these reasons and because of the constant density consideration, natural convection will be neglected, hence the continuity and momentum equations will not be considered. This is expected to have a low impact on the quality of the results, since the diameter, length of the tube and fin fraction follow the trend suggested by Vogel and Johnson (2019) to have a diffusive-dominated heat transfer. For the same reasons, buoyancy effects are also neglected as previously proposed by Sciacovelli et al. (2015).
The following mathematical description of the model can be found on COMSOL's Heat Transfer Module documentation (COMSOL-Multiphysics®). The energy equation is solved with the PCM properties calculated based on the apparent heat capacity formulation. A temperature glide of 2 K between solid and liquid is considered instead of adding the latent heat of fusion to the energy equation.

2.2 Finned profiles characterization

If the hexagonal enclosure, the finned tube, and the PCM are discretized using elements of width Δx and height Δy, a distance function $D_{min}(x, y)$ calculating the minimum distance of each of the PCM elements to its nearest fin element can be defined. This can be seen for a coarse mesh configuration in Figure 4:

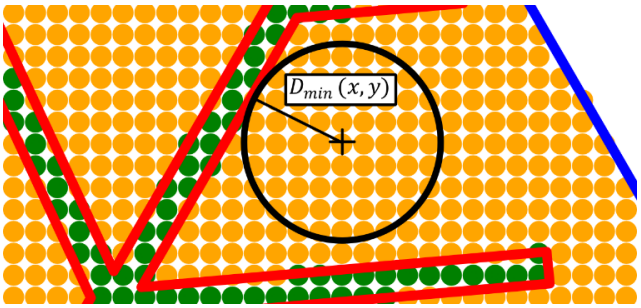

Figure 4: Concept for the minimum distance function implemented in Python using a coarse mesh.

To compare the different fin profiles, an average value of this function AD_{min} can be calculated as shown in Equation (2). This term is presented to systematically quantify the paths each fin profile imposes on the heat transfer problem and compare the four geometric structures. In principle, the shorter these distances, the shorter the paths, and therefore the time required for phase change.

$$AD_{min} = \frac{1}{n}\sum_{i=1}^{n} D_{min}(x,y) \tag{2}$$

Figure 5 shows the results of the distance from every PCM element to the nearest fin element (Heat Transfer Surface). As expected, the fins with an even distribution of the material, such as the 24-Branch-Star or the TESIN fin profile had distances up to 6 mm, whereas the profile with the most concentrated distribution, the 6-Branch-Star fin profile, had a wider distance spectrum, with its maximum near 18 mm. In almost all cases, the colormap resembles the paths the phase change follows.

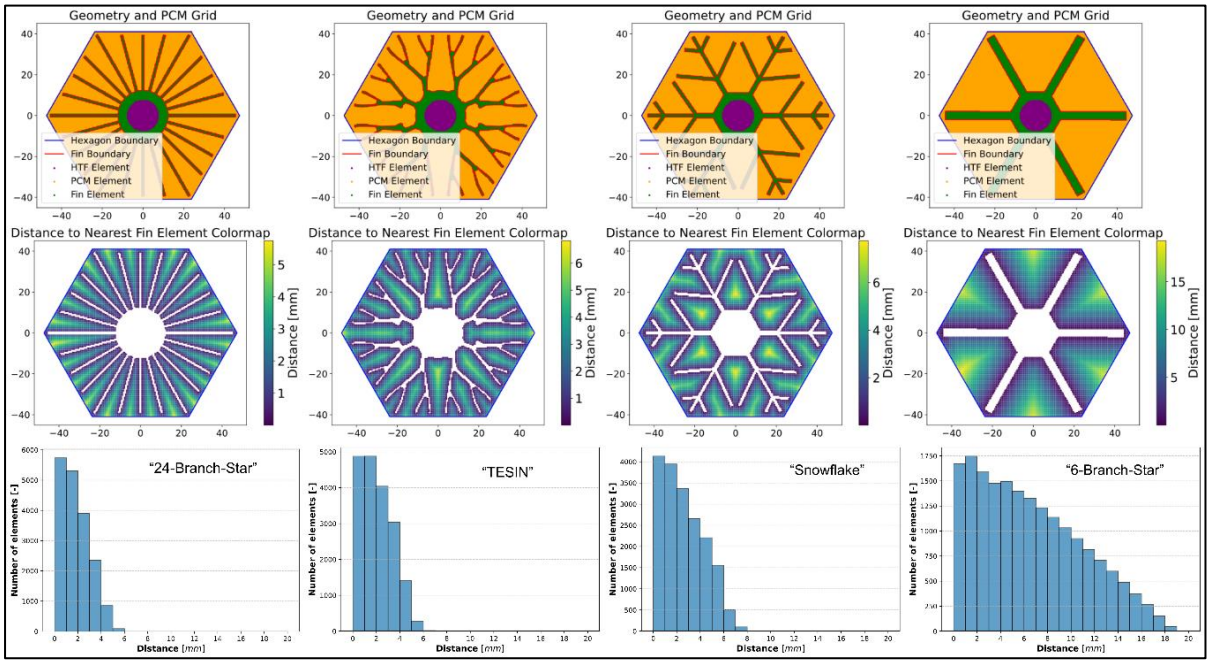

Figure 5: Distance to the nearest finned structure for each fin design.

Table 3 shows the results of the characterization. As previously stated, all the fin profiles have the same cross-sectional area and fin fraction but differ in the aluminum distribution. Tube and hexagon radii are also common for all profiles. The average minimum distance, fin perimeter (contact area between PCM and Fin divided by its height), as well as the melting and solidification times, are included in the table.

Table 3: Results of the characterization of the fin profiles.

Fin Profile	24-Branch Star	TESIN	Snowflake	6-Branch-Star
A_{fin} $[mm^2]$	770			
f_{fin} [%]	13.2			
Tube internal radius [mm]	8			
Tube external radius [mm]	12.326			
Hexagon internal radius [mm]	41			
Hexagon external radius [mm]	47.34			
PCM and tube height [mm]	15			
Fin perimeter [mm]	1480	1291	1078	463
AD_{min} [mm]	1.80	2.06	2.60	6.49
Solidification time [s]	1100	1355	1845	5785
Melting time [s]	1130	1355	1885	5785

3 RESULTS

Figure 6 shows the results of the liquid fraction of the PCM and the heat flux at a given time calculated for the four different fin geometries. In the label, it is also shown the contact perimeter (in mm) between PCM and fins for each geometry. It can be seen that the larger the contact perimeter between the respective fin and PCM, the faster the phase change occurs.

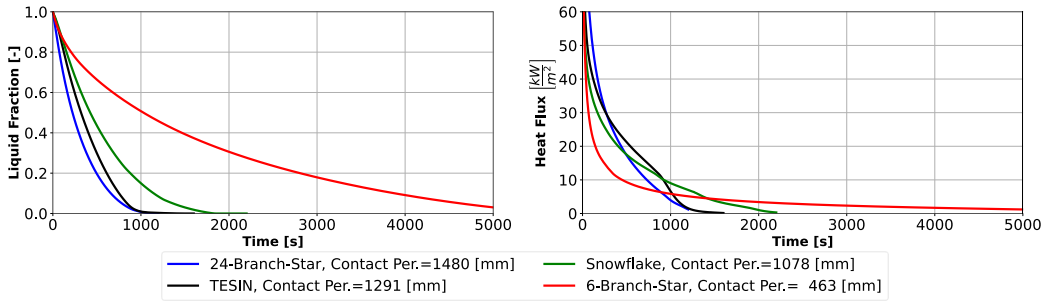

Figure 6: Solidification liquid fraction and heat flux for each of the fin profiles.

Figure 7 shows the same results plotted in Figure 6 but for the melting process. The melting behavior for each fin geometry follows the same tendency as in the solidification process case but with negative signs.

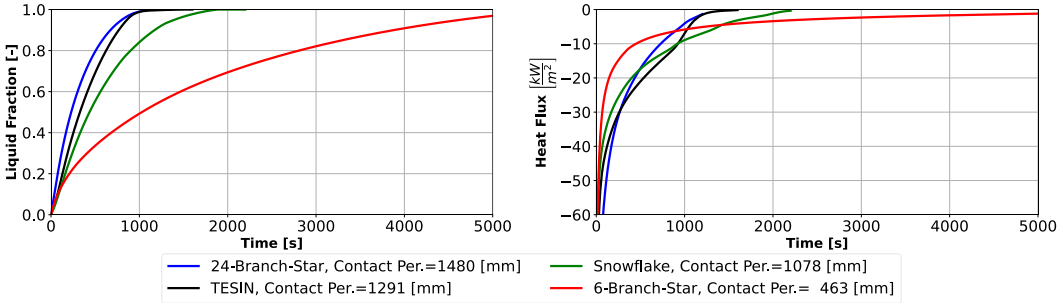

Figure 7: Melting liquid fraction and heat flux for each of the fin profiles.

Figure 8 shows the comparison of the finned profiles during phase change. Because of the assumptions used in this study, the melting and solidification curves have virtually the same results of heat flux over the liquid fraction. This approach, analyzing heat flux at a given liquid fraction instead of time, allows a straightforward comparison among the different fin geometries. Here, the fin with the largest contact

perimeter (24-Branch-Star) shows the highest overall heat flux, nevertheless, intermediate profiles, such as the TESIN (black) and Snowflake (green) have a flatter discharge curve, which would be required depending on the application.

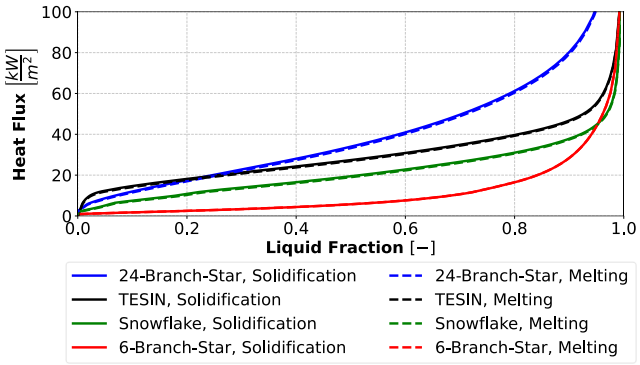

Figure 8: Heat flux comparison during phase change.

Figure 9 shows the correlation of both parameters, contact perimeter and AD_{min}, over the melting time. Since the phase transitions require nearly the same time, only the melting time was considered for the evaluation. Linear regressions were calculated for both parameters, showing a relatively high correlation for the contact perimeter, and a directly proportional relation to the average minimum distances.

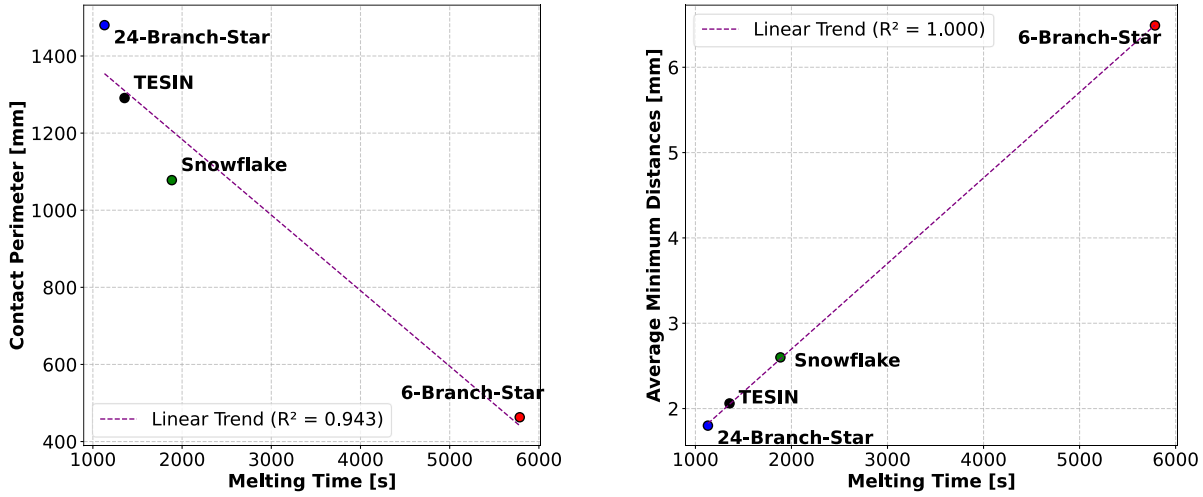

Figure 9: Tendencies found for the proposed parameters with respect to the melting time.

Although the D_{min} map can give insights into the path the phase change front will follow during solidification and melting, additional parameters are required to fully characterize the different fin profiles. Since the temperature of the fin's elements has a temperature gradient depending on their distance to the inner tube boundary, their surface can't be assumed as isothermal. Furthermore, two points could have the same minimum distance to a given fin element but if additional fin elements are neighboring it, the PCM elements would receive heat flows from more than one source, resulting in different melting times. This was the case for the TESIN and Snowflake profiles. Although there is a relatively high correlation for both of the proposed parameters, more geometries are required to fill the gap between the snowflake and the 6-branch-star profiles. Hence, the next task to develop the multi-scale simulation tool shown in Figure 2, is the parametrization of the finned geometries to numerically analyze if the correlation shown in Figure 9 is valid for a wider variety of designs. Then the fins could be parametrically optimized following the residual energy minimization approach proposed by Pizzolato et al. (2017b). Furthermore, the resulting geometric parameters show a great potential to build a simplified model of the melting and solidification of LHTES using finned structures. Such a geometrically based Blackbox model would be an improvement with respect to current approaches

which require either CFD or experimental results for their calibration, and thus would expand the range of possible configurations on the LHTES, currently limited to a short number of fin profiles on the storage level assessment.

4 CONCLUSIONS

The characterization of finned tube heat exchangers used in LHTES systems to enhance the low-conductive PCMs is crucial for the development of accurate simulation tools.

- The contact perimeter tendency showed that the greater the contact area between PCM and fins, the shorter the time required for phase change.
- The innovative parameter of the Average Minimum Distances (AD_{min}) between PCM and fins was calculated, showing a linear correlation with the melting and solidification time. The challenges of the new parameter were discussed, considering it to be a promising alternative to characterize fin profiles.
- Future work will be done on the parametrization of finned geometries to study if the correlations shown in this paper apply to a wider range of designs. Subsequently, a parametric optimization of the finned structures could be carried out using a minimization of the residual energy of the storage.

DECLARATION OF AI-ASSISTED TECHNOLOGIES

DeepL and Grammarly were used to improve the readability, grammar and language of this article.

NOMENCLATURE

Symbols & Abbreviations

A	Area	[m^2]
D	Distance	[mm]
AD_{min}	Average Minimum Distances	[mm]
f	Fraction	[%]
HTF	Heat Transfer Fluid	
LHTES	Latent Heat Thermal Energy Storage	
PCM	Phase Change Material	

Subscripts

fin	Fin
hex	Hexagon
PCM	PCM
tube	Tube

REFERENCES

COMSOL-Multiphysics®. (2025). (Version 6.3) COMSOL AB. **www.comsol.com**

DLR. (2012). *Entwicklung und Integration Thermischer Energiespeicher in Rinnenkraftwerken mit Solarer Direktverdampfung: Verbundvorhaben ITES-Schlussbericht*.

Dumont, O., Frate, G. F., Pillai, A., Lecompte, S., De paepe, M., & Lemort, V. (2020). Carnot battery technology: A state-of-the-art review. *Journal of Energy Storage*, *32*. https://doi.org/10.1016/j.est.2020.101756

Ge, R., Humbert, G., Martinez, R., Attallah, M. M., & Sciacovelli, A. (2020). Additive manufacturing of a topology-optimised multi-tube energy storage device: Experimental tests and numerical

analysis. *Applied Thermal Engineering*, *180*. https://doi.org/10.1016/j.applthermaleng.2020.115878

IEA. (2024). *Batteries and Secure Energy Transitions*. https://www.iea.org/reports/batteries-and-secure-energy-transitions

Li, Z., Lu, Y., Huang, R., Chang, J., Yu, X., Jiang, R., Yu, X., & Roskilly, A. P. (2021). Applications and technological challenges for heat recovery, storage and utilisation with latent thermal energy storage. *Applied Energy*, *283*. https://doi.org/10.1016/j.apenergy.2020.116277

Mehling, H. C., Luisa. (2008). *Heat and cold storage with PCM*. https://doi.org/10.1007/978-3-540-68557-9

Pizzolato, A., Sharma, A., Maute, K., Sciacovelli, A., & Verda, V. (2017a). Design of effective fins for fast PCM melting and solidification in shell-and-tube latent heat thermal energy storage through topology optimization. *Applied Energy*, *208*, 210-227. https://doi.org/10.1016/j.apenergy.2017.10.050

Pizzolato, A., Sharma, A., Maute, K., Sciacovelli, A., & Verda, V. (2017b). Topology optimization for heat transfer enhancement in Latent Heat Thermal Energy Storage. *International Journal of Heat and Mass Transfer*, *113*, 875-888. https://doi.org/10.1016/j.ijheatmasstransfer.2017.05.098

Sciacovelli, A., Gagliardi, F., & Verda, V. (2015). Maximization of performance of a PCM latent heat storage system with innovative fins. *Applied Energy*, *137*, 707-715. https://doi.org/10.1016/J.APENERGY.2014.07.015

Steinmann, W.-D. (2022). *Thermal Energy Storage for Medium and High Temperatures*. https://doi.org/10.1007/978-3-658-02004-0

Tay, N. H. S., Belusko, M., & Bruno, F. (2012). An effectiveness-NTU technique for characterising tube-in-tank phase change thermal energy storage systems. *Applied Energy*, *91*(1), 309-319. https://doi.org/10.1016/j.apenergy.2011.09.039

Vandersickel, A., Gutierrez, A., Vasta, S., Engelbrecht, K., Ma, Z., Ding, Y., & Bollinger, B. (2023). *IEA Task 36 Carnot Batteries Final Report*.

Vogel, J., & Johnson, M. (2019). Natural convection during melting in vertical finned tube latent thermal energy storage systems. *Applied Energy*, *246*, 38-52. https://doi.org/10.1016/j.apenergy.2019.04.011

Vogel, J., Keller, M., & Johnson, M. (2020). Numerical modeling of large-scale finned tube latent thermal energy storage systems. *Journal of Energy Storage*, *29*. https://doi.org/10.1016/j.est.2020.101389

Wang, Y., Zadeh, P. G., Duong, X. Q., & Chung, J. D. (2023). Optimizing fin design for enhanced melting performance in latent heat thermal energy storage systems. *Journal of Energy Storage*, *73*. https://doi.org/10.1016/j.est.2023.109108

Zayed, M., Zhao, J., Li, W., Elsheikh, A., Elbanna, A., Jing, L., & Geweda, A. (2020). Recent progress in phase change materials storage containers: Geometries, design considerations and heat transfer improvement methods. *Journal of Energy Storage*, *30*, 101341. https://doi.org/10.1016/j.est.2020.101341

Zhang, S., Mancin, S., & Pu, L. (2023). A review and prospective of fin design to improve heat transfer performance of latent thermal energy storage. *Journal of Energy Storage*, *62*. https://doi.org/10.1016/j.est.2023.106825

Zhu, T., Zhang, Y., Lu, X., Zhang, W., & Fengdi. (2023). A Review on Heat Transfer Enhancement of Phase Change Materials Using Fin Tubes. *Energies*. https://doi.org/10.3390/en16010545

ACKNOWLEDGEMENT

Authors acknowledge the financial support given by the German Research Foundation (DFG) Priority Program: "Carnot Batteries: Inverse Design from Markets to Molecules" (SPP 2403). The first Author is grateful to Jonas Tombrink, Tatjana Janzen, Sabri Bekgöz, and Simon Ruwe for the inspiring discussion regarding fin characterization and LHTES modeling.